HHS Public Access

Author manuscript

Structure. Author manuscript; available in PMC 2018 July 05.

Published in final edited form as:

Structure. 2017 July 05; 25(7): 1068–1078.e2. doi:10.1016/j.str.2017.05.015.

Crystal structure of chicken γS-crystallin reveals lattice contacts with implications for function in the lens and the evolution of the βγ-crystallins

Vatsala Sagar[1], **Sumit K. Chaturvedi**[2], **Peter Schuck**[2], and **Graeme Wistow**[1,*]

[1]Section on Molecular Structure and Functional Genomics, National Eye Institute, National Institutes of Health, Bethesda, Maryland, United States of America

[2]Dynamics of Macromolecular Assembly Section, LCIMB, National Institute of Biomedical Imaging and Bioengineering, National Institutes of Health, Bethesda, Maryland, United States of America

Summary

Previous attempts to crystallize mammalian γS-crystallin were unsuccessful. Native L16 chicken γS crystallized avidly while the Q16 mutant did not. The x-ray structure for chicken γS at 2.3Å resolution shows the canonical structure of the superfamily plus a well-ordered N-arm aligned with a β-sheet of a neighboring N-domain. L16 is also in a lattice contact, partially shielded from solvent. Unexpectedly, the major lattice contact matches a conserved interface (QR) in the multimeric β-crystallins. QR shows little conservation of residue contacts, except for one between symmetry-related tyrosines, but molecular dipoles for the proteins with QR show striking similarities while other γ-crystallins differ. In γS, QR has few hydrophobic contacts and features a thin layer of tightly bound water. The free energy of QR is slightly repulsive and AUC confirms no dimerization in solution. The lattice contacts suggest how γcrystallins allow close packing without aggregation in the crowded environment of the lens.

eTOC

The crystal structure of γS-crystallin shows how proteins in the eye lens can form non-binding contacts with low hydration without aggregation. Monomeric γS also forms an intermolecular interface very similar to one in dimeric β-crystallins: few contacts are conserved but molecular dipoles have similarities.

*To whom correspondence should be addressed: Lead Contact. Graeme Wistow, Ph.D., Section on Molecular Structure and Functional Genomics, National Eye Institute, Building 6 Room 106, National Institutes of Health, Bethesda, MD, USA., Tel: 301-402-3452; graeme@helix.nih.gov.

Author Contributions

VS performed crystallographic experiments and VS and GW analyzed the structure data. SKC performed AUC experiments and SKC and PS analyzed the data. All authors discussed results and approved the manuscript, which was mainly written by GW and VS.

Supplemental Information

Supplemental Table S1

Supplemental Table S2

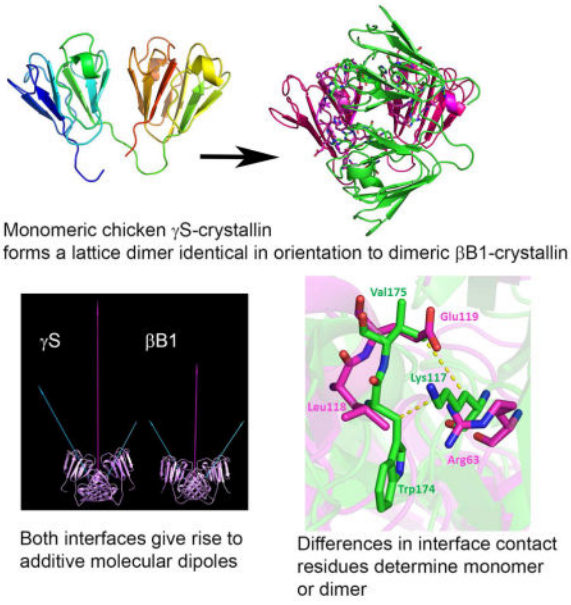

Keywords

Crystallin; lens; non-bonding interfaces; dimerization; molecular dipoles

Introduction

γ-Crystallins are major structural proteins of the vertebrate eye lens (Slingsby and Wistow, 2014; Slingsby et al., 2013). They are particularly abundant in lenses of fish and rodents, those with the highest protein concentrations, hence the sharpest refractive index gradients, and in the central, densest, nuclear regions of lenses in other mammalian species. They are thought to be evolutionarily adapted for the conditions of high molecular crowding necessary for the refractive properties of the lens and for a role in maintaining the short range order of lens cytoplasm required for transparency (Delaye and Tardieu, 1983; Zhao et al., 2011b). Indeed, we have previously shown that these monomeric proteins are highly compact, with very low frictional ratios in solution (Chen et al., 2014; Zhao et al., 2014).

The γ-crystallin family includes members that are specific to different taxa, such as fish and mammals, and some that are represented throughout vertebrates (Wistow et al., 2005). Prominent among the latter class is γS-crystallin. Indeed, although it had long been thought that γ-crystallins were absent from the relatively soft, flexible lenses of birds, we have shown that birds do express γS, albeit at a lower level than in many other groups (Chen et al., 2016). Although chicken γS is a well-conserved member of the family, we noticed one unusual residue substitution which replaced a glutamine in the first of the four repeated Greek key motifs of the protein with leucine (L16 in the chicken sequence and all other predicted avian sequences, from falcon to hummingbird). The Greek key motif found in γ-crystallins and in the related β-crystallins has a sequence signature with conservation of some key residues. However, little attention has been paid to the conserved glutamine and the reason for its conservation throughout βγ-crystallins is unknown.

The surface properties of γ-crystallins are very important for solubility and substitutions of single residues can have major effects, as for example in the case of the P23T mutation in human γD (Evans et al., 2004). However, we found no evidence for any differences in solubility or stability for chicken γS with the native (non-conservative) L16 or with substituted Q16 (Chen et al., 2016). However, we reasoned that L16 could still have effects on protein interactions.

While many β- and γ-crystallins have been crystallized, γS has proved recalcitrant. Previous efforts to crystallize human and mouse γS did not succeed and when separate N- and C-terminal domains of human γS were used, only the isolated C domain crystallized (Purkiss et al., 2002). However, it was possible to determine the monomer structure of intact mouse γS by NMR (Wu et al., 2005). Here we report that, in contrast to other orthologs that have been tested, wild type chicken γS crystallizes avidly, while the Q16 mutant does not, allowing the first determination of a crystal structure for a γS and the examination of some informative crystal lattice contacts.

Results

Crystal structure

Both L16 (wild type) and Q16 chicken γS were purified and screened over 288 crystallization conditions. No crystals were obtained for Q16. In contrast, L16 produced crystals in 45/288 (16%) of the conditions tested (Table S1) over a wide range of pH (5.5–9.5), salts and precipitants, even including 72% w/v glycerol, and at a protein concentration of only 0.125 mg/ml. (Some of these conditions produced needles and space groups were not determined for all conditions). After optimization, diffraction quality crystals were grown in 0.2 M Ammonium acetate pH 7.1 and 16% PEG 3350 at room temperature over 4 days, although most of these were twinned. Crystals were large enough to collect a 2.3Å data set using a rotating anode x-ray generator (Table 1).

The structure of native chicken γS was solved by molecular replacement using the coordinates of mouse γS derived from solution NMR (Wu et al., 2005), substituting Gly for non-matching side chains. (Fig 1a). There was one molecule in the asymmetric unit. It has the familiar canonical structure, with two similar domains each formed from a pair of similar modified Greek Key motifs (consisting of four β-strands: *a-d*), connected by a linker peptide. The refined structure matched the mouse γS solution structure (1ZWAO) with RMSD of 2.1Å for 1311 atoms excluding the N-terminal arms, and had a slightly closer match to the crystal structure of human γD crystallin (1HKO) with RMSD of 1.9Å for 1172 atoms. These differences likely reflect the constraints of a crystal, as opposed to a free solution structure. One difference in chicken γS is A128, at the start of the *d* strand of the third motif, which replaces a well-conserved serine residue involved in the characteristic folded structure of the strand *a-b* hairpin found in each repeated motif of the βγ-crystallin superfamily. This S/A substitution has no obvious effect on local structure in chicken γS and does not seem to have any noticeable destabilizing effect on the protein (Chen et al., 2016); furthermore the same substitution is also found in γN-crystallins (Wistow et al., 2005).

L16 is located at the tip of the folded strand *a-b* hairpin of motif 1 (Fig 1a). The presence of L16 instead of the glutamine which is conserved in other members of the family had no effect on the local conformation of the protein backbone in chicken γS compared with that in mouse γS, and the side chains of the equivalent L/Q16 residues have very similar orientations, even though one is polar and the other is non-polar (Fig 1b).

Lattice contacts

Crystal lattice contacts for chicken γS as defined by PISA (Krissinel and Henrick, 2007) are shown in Table 2. L16 participates in one of these contacts with an area of 390Å^2. This includes several intermolecular polar interactions between the N-domain of one monomer and a neighboring C-domain (Fig 2). L16 inserts between the folded β-hairpin of the *a* and *b* strands of motif 3 and the *c-d* loop of motif 4 in the neighboring monomer. L16 itself does not make a direct hydrophobic contact, but is significantly shielded (69%) from solvent in the crystal lattice (solvent accessible area for L16 in isolated monomer =107Å^2, reduced to 33Å^2 in the crystal lattice) which presumably contributes to crystallization in this space group.

Another lattice contact involves the N-arm which (in contrast with that of the mouse γS NMR structure which exhibits a high degree of structural freedom) is relatively well-defined in the crystal structure (Fig 3A), with low to moderate B-factors for residues 2–4 (all below 50 Å^2). The 4 residues of the N-arm extend away from the N-domain and residues 2–4 line up with the edge of the outer β-sheet of a neighboring N-domain (strand *b* of the first motif), almost forming a fifth strand of the sheet (Fig 3A, B). There is one main chain backbone hydrogen bond interaction, between the peptide carbonyl of R2 and the peptide nitrogen of the adjacent Q21′ while a second interaction between G4 and R19′ is bridged by water. The side chain of R2 forms an ion-pair with D23′ of the other monomer and is within hydrogen bonding distance of Y20′. While the N-arm of γS in solution may be relatively disordered, the crystal structure shows that in crowded conditions this structure can adopt a much more ordered conformation, aligned with a β-sheet.

In addition to typical lattice contacts with limited interaction areas, the crystal also contains a very large lattice contact between adjacent monomers (Fig 4A, B). The contact area defined by PISA is 852Å^2, 9.3% of the monomer surface area. For comparison, this is ~50% larger than the largest lattice contacts in human γD (PDB: 1HKO) or γB crystals (PDB: 2JDF). Despite this, the free energy of the interaction is positive, ΔG = 4.7kcal/mol, inconsistent with dimerization. This can be explained by a lack of hydrophobic contacts between monomers. Most of the contact area consists of surface polar side chains which have extensive intramolecular contacts, some direct intermolecular contacts and other contacts, both intra- and inter-molecular, involving water bridges (Fig 4). Thus, the interface, although extensive, involves little attractive interaction between monomers.

The networking of surface polar side chains with intramolecular hydrogen bond and charged interactions is a general feature of γ-crystallins and was noticed in the first such structure to be examined (Blundell et al., 1981; Wistow et al., 1983). This internalization of polar bonding potential is thought to reduce the requirement for solvation by bulk water. Chicken γS, follows the same general pattern, with most of the solvent-exposed side chains outside

the lattice contacts forming intramolecular interactions. In the large lattice contact, polar side chains are also oriented towards each other in a similar kind of network, but the structure also shows well-defined water molecules apparently coordinated between surface side chains, while others are coordinated by side chains across the lattice contact, forming intermolecular bridges (Fig 4B, C). This has the effect of producing a thin layer of bound water between the monomers, satisfying solvation without the formation of tight intermolecular binding.

Unexpectedly, the lattice dimer of chicken γS is very similar to a dimer interface found in all crystal structures determined for the related, multimeric β-crystallins (Slingsby and Wistow, 2014; Van Montfort et al., 2003) in which it was designated QR, (based on the symmetry in the original βB2 structure (Bax et al., 1990) (Fig 5). For the multiple structure alignment shown in figure 5F, G, the RMSD from chicken γS is 4.9Å for 2338 atoms for βB1 (PDB: 1OKl), 5.8Å for 977 atoms for βB2 (PDB: 1YTQ) and 4.2Å for 2196 atoms for βA4 (PDB:3LWK). The orientation of this interface is highly conserved, but its extent and predicted free energies vary: in some structures, it appears to be a true dimer interface while in others it is a lattice contact only. In the crystal structure for βB1, truncated through deletion of N-arm and C-terminal extension (Van Montfort et al., 2003), the QR interface has an area of 1571 Å2 and ΔG = −5.6 kcal/mol and is responsible for solution dimerization (Bateman et al., 2001). In the crystal structure of βB2, dimerization occurs through domain-swapping (Bax et al., 1990; Lapatto et al., 1991), but in the crystal lattice, dimers interact through the common QR interface to form a non-bonded lattice tetramer (Bax et al., 1990; Lapatto et al., 1991; Smith et al., 2007) (Fig 5). Surprisingly, a very recent study has suggested that, in solution, human βB2 forms a compact dimer thought to be a QR-based dimer without domain swapping (Xi et al., 2017). As yet, there are no coordinates for this structure. We built a simple QR dimer model, using the QR interaction from the βB2 crystal lattice tetramer and substituting the connecting peptide conformation of βB1. However, the PISA predicted energy of dimerization for the model was slightly positive, ΔG = 1.7 kcal/mol while the predicted energy of dissociation (ΔGdiss) was −9.5 kcal/mol. This suggests that our model does not correspond to the compact dimer thus making it difficult to draw any conclusions. In truncated βB3, a somewhat modified version of the interface is involved in trimer formation (Fig 5C). In truncated βA4, it is again involved in dimerization and formation of octamer complexes.

Figure 6 shows a sequence alignment for chicken γS compared with those for human βB1, βB2 and βA4 for which crystal structures show the presence of QR interfaces (βB3 is omitted to limit the comparison to the most similar QR interfaces in monomer-monomer or dimer-dimer structures). Residues of the QR interface defined by the Contact program are shown. In chicken γS, the contacts of the QR interface are found in two stretches of sequence located in motifs 2 and 4. These are the most highly conserved motifs and are the main contributors to the interdomain contact in the monomer: the residues involved in QR are distinct from the interdomain contact. Figure 6 indicates the residues with side-chain interactions in the interface (rather than only main chain interactions). These are residues: R62, Y66, H70, H71, M73 and L75 in the strand *c*-*d* region of the second motif; H141, N143, Y144 and R145 in the strand *a* region of the fourth motif. A single residue in the *d* strand of motif 4, R173, also forms a contact (to N143). The equivalent regions in the β-

crystallins are also involved in the QR interface, but include additional residue contacts. The β-crystallins also have additional contact side chains in the strand *c-d* region of motif 3 and strand *d* of motif 4. Some of these residues are also conserved in chicken γS, but do not form contacts, while some of residues in the robust β-crystallin interfaces, such as W174 in βB1, which have significant hydrophobic contacts are lacking in γS (Fig 6A).

We looked for a minimal set of conserved interactions that might define the QR contact in the crystal lattice. However, comparison of the crystal structures showed that even some conserved residues in in the contact regions form different interactions in different structures. For example, the conserved residues R145 in γS and R201 in βB1 are both involved in the QR interface, however the side chains have different conformations so that R145 interacts with the side chain of H71 and the main chain of E65, while R201 interacts with main chain atoms of W126 and I114 (Fig 6B). Remarkably, only one residue appears to be conserved and to form the same interaction among all the structures for the QR interface: Y144 (in γS) and its equivalents form a well-conserved side-by-side Van der Waals contact in all structures along the two-fold axis of the interface (Fig 6C). This residue is part of the conserved folded β-hairpin between *a* and *b* strands of the fourth motif of these proteins. Flanking residues are involved in the interface, but the specific interactions vary among the proteins.

Since the conservation of the QR interface does not involve well-conserved side chain interactions, we considered the idea that some overall property, such as molecular dipoles, might play a role in the association of monomers. Differences in molecular dipoles for γ-crystallins have been noticed previously (Norledge et al., 1997; Purkiss et al., 2007) and the general role of dipoles in protein homodimer formation has been discussed (Campbell et al., 2014). As shown in Fig 7, monomers of chicken γS and βB1 have dipoles of similar magnitude, oriented from the interdomain interface at a similar angle through the N-domain. In the crystal dimer, these dipoles add to create a larger magnitude dipole through the QR interface. βA4 has a different monomer dipole but in the dimer, this too produces a larger molecular dipole through the QR interface, although opposite in direction to that in the other two proteins. Since the domain swap in the crystal structure of βB2 complicates the calculation of monomer and dimer dipoles (because N- and C-domains of the QR interface are not parts of the same polypeptide chain) this was not considered. No coordinates are available for the recently described compact solution dimer for this protein (Xi et al., 2017).

We then used modelling to place other crystallographically determined γ-crystallin structures in the same positions as the γS QR dimer. Monomer dipoles for mouse γC, human γD and bovine γE and γF had different orientations from γS and in the modelled dimer configuration did not produce the increased molecular dipole along the same axis through QR. This correlation is consistent with the idea that additive molecular dipoles might indeed contribute to the alignment of γ and β monomers to form QR. The same modelling exercise for human γB did produce an increased, similarly aligned dipole in the modelled dimer; however, the dipoles of isolated monomers did not follow the QR pattern and were aligned toward each other in the model, which might prevent approach of the monomers in this QR configuration

Although the calculated free energy of the QR interaction in chicken γS is not by itself consistent with dimer formation, recent results have described solution dimer formation for human γS-crystallin, including involvement for the N-arm (Ray et al., 2016) while another study described a small fraction of the protein associating into clusters (Mohr et al., 2013). We investigated the behavior of chicken γS in solution using analytical ultracentrifugation.

Analytical Ultracentrifugation

Sedimentation equilibrium experiments were carried out at concentrations between 2.3 – 17 μM at 4 °C. A single species model described the data well within the noise of data acquisition (Figure 8A). The best-fit molar mass of 20.2 kDa is within typical errors in the partial-specific volume consistent with the monomer sequence molar mass.

To assess dimerization at higher concentrations, sedimentation velocity (SV) experiments were carried out (Figure 8B, C, D). At moderate concentrations the sedimentation coefficient distributions distribution showed a single peak with $s_{20w,0}$ of 2.31S, indicating a highly compact monomer with a frictional ratio of 1.24, slightly above the previously measured value of 1.21 for mouse γS (Zhao et al., 2014). Even at the highest concentration studied, only a single peak in the sedimentation coefficient distribution was observed. This concentration, 24mg/ml, exceeds the likely effective concentration of γS in the chicken lens, where it is a minor component of the total crystallin (Chen et al., 2016). The s-value slightly decreased with concentration, which is a signature of obligate hydrodynamic non-ideality (Figure 8C). Dimerization with KD in the mM range or weaker could be masked by this decrease, but unfortunately, its estimate is confounded by correlation with the assumptions on the magnitude of hydrodynamic repulsive interactions, and the dimer s-value. Using theoretical values for the non-ideality of a non-interacting hydrodynamically equivalent sphere, and the constraint of the dimer s-value to fall within 1.4 – 1.6-fold the monomer s-value, a best-fit Kd of 4.6 mM (95% CI from 2.6 – 10.2 mM) was estimated (Figure 8D). However, an alternative interpretation of the data can be made without any dimerization but allowing for slightly attractive interactions modulating the protein distance distributions in solution.

These results confirm that despite its ability to form an extensive intermolecular interaction in the crystal lattice, chicken γS shows no clear evidence for multimerization even at high concentration and that the presence of L16 does not contribute to enhanced non-covalent interactions in solution.

Discussion

Crystallins are highly specialized for their role in creating a transparent, refractive lens for the vertebrate eye (Slingsby and Wistow, 2014; Slingsby et al., 2013). In particular, γ-crystallins seem to be highly adapted for the lens role, with very compact, monomeric structures, allowing for tight packing, (Chen et al., 2014; Zhao et al., 2014), good thermodynamic stability, allowing for extreme longevity, and even unusual amino acid compositions, selected for their contributions to refractive index (Mahendiran et al., 2014; Zhao et al., 2011a). While γ-crystallins are monomers, the structurally related β-crystallins form dimers and higher multimers both *in vitro* and in *vivo* (Slingsby et al., 2013).

Intermolecular interactions of crystallins are important for their functions, but the determinants of these interactions in the lens cytoplasm are still not well-understood.

Several γ-crystallins have been crystallized, allowing for detailed structural studies, however previous attempts to crystallize mammalian γS were unsuccessful and led only to the crystallization of the isolated C-domain of human γS while the complete protein and isolated N-domain did not crystallize (Basak et al., 1998). This failure to crystallize has been attributed to repulsive interactions in γS (Pande et al., 2015; Tardieu et al., 1992).

Although birds were long thought to lack all γ-crystallins, we recently showed that γS is present in birds, and found that chicken γS is expressed in the lens, although at relatively low levels (Chen et al., 2016). The primary sequence of avian γS is well conserved with that seen in other vertebrates. However, we noticed that throughout the birds there is a substitution of a residue that is highly conserved in both β- and γ-crystallins throughout the other vertebrates. This is at position 16 in the chicken γS sequence, where the residue is leucine instead of the otherwise conserved glutamine. The reason for the conservation of Q16 and its equivalent positions in other members of the family is not known. We also found no evidence for any structure, solubility or stability differences between native L16 chicken γS and the engineered Q16 version. However, as shown here, we found a remarkable difference in the crystallization of the two proteins, with L16 crystallizing easily under many conditions while Q16, like its mammalian orthologs, failed to produce crystals. The crystal structure for chicken γS shows that L16 is significantly shielded from water by a lattice contact in the crystal. This provides some rationale for crystallization of the native protein.

Crystal lattice contacts also provide some insight into ways in which γS may interact with other crystallins in the crowded conditions of the lens. The short N-arm, which shows high mobility in the solution NMR structure of mouse γS (Wu et al., 2005) is well defined in the crystal and is involved in a lattice contact in which it at least partially aligns with the edge of a β-sheet of another N-domain. γA-F crystallins lack N-arms, but short N-arms are present in γS and γN while in the related β-crystallins they can be much longer (Slingsby et al., 2013; Wistow et al., 2005). The role of N-arms in βγ-crystallins is not clear; they could participate in formation of multimers, they could also provide an entropic contribution to solubility by freely moving in solution. The chicken γS structure shows that under crowded conditions extensions can also be involved in well-ordered interactions between crystallins.

The γS crystal structure also contains a large lattice contact (about 50% larger than in other γcrystallin crystal structures). This contact region contains few hydrophobic contacts and a small number of direct intermolecular contacts between polar side chains. Indeed, the calculated free energy of the interaction is slightly repulsive. Within the contact region, surface polar side chains participate in intramolecular contacts that include tightly bound waters, coordinated between one or more side chains. often forming intermolecular bridges. The overall effect is of relatively limited direct interaction between the protein monomers while polar interactions are satisfied by a layer of tightly bound waters.

This suggests a model for the way in which γ-crystallins may associate with other crystallins (Slingsby and Wistow, 2014; Slingsby et al., 2013) and other components of the

lens (Fan et al., 2012) in an environment with low water content and a high degree of molecular crowding. Similar packing to that seen in the γS-crystal would allow very close contact without multimerization or aggregation and with the involvement of little water to satisfy polar interactions. Indeed, AUC measurements confirm that chicken γS shows little tendency to multimerize, even at high concentrations. The data are consistent with slightly attractive interactions, but with values very similar to those previously reported for mouse γS (Zhao et al., 2014).

Although the large γS lattice contact illustrates ways in which γ-crystallins can interact without multimerizing, it is remarkably similar to a conserved interface involved in the multimerization of the β-crystallins in solution or in crystals. All the crystal structures for β-crystallins contain this interface, called QR, which is more or less robustly involved in same-protein interactions in different members of the family (Van Montfort et al., 2003; Xi et al., 2017). Its prevalence suggests that the QR interface is an ancestral feature of the β-crystallins and so might also be ancestral for the related γ-crystallins. The idea that γ-crystallins evolved from the structurally related β-crystallins is supported by gene structures in the two families (Kappe et al., 2010; Wistow, 2012). In the genes for β-crystallins, each of the four repeated Greek Key motifs is encoded in a single exon and the same pattern is seen in the genes of the AIM1 family, vertebrate members of the βγ-crystallin superfamily with non-lens roles (Ray et al., 1997; Teichmann et al., 1998; Wistow, 2012). In contrast, the genes for γS and for other γ-crystallins, such as the γA-F family in mammals, have lost the introns that separate the motif-encoding exons of each domain, while the gene structure for the intermediate γN-crystallin has one domain encoded like a β-crystallin and one like a γ-crystallin (Kappe et al., 2010; Wistow et al., 2005), suggesting a transition in exon structure from β- to γ-crystallin families. Interestingly, γS itself was originally designated as βs (for electrophoretically “slow”) when isolated from cow lens extracts (Quax-Jeuken et al., 1985).

This suggests that the evolution of monomeric γ-crystallins from multimeric β-crystallins may have occurred at least partly through modifications of the QR interface which reduced the potential for dimerization. Even so, γS retains the ability to form the same intermolecular alignment, at least in the crystal lattice. The QR contact depends on residues in the second and fourth motifs of the structure, so that the interface brings the interdomain contact regions, and thus the centers of gravity of two monomers, close together. Surprisingly only one residue, Y144, part of the folded β-hairpin structure of the fourth motif, is completely conserved in identity and conformation in QR in γS and the β-crystallins. Other residues have changed identity or, if conserved, form different interactions. With so little conservation, it is hard to determine why γS forms the QR interface. One possibility is that β- and γ-monomers align in this configuration because of some overall characteristic, such as their molecular dipoles. Indeed, we found that the proteins known to form the QR interface crystallographically have monomeric molecular dipoles that align in the dimer to give rise to a larger dipole oriented perpendicular to the QR interface. This seems to fit general observations for homodimer formation (Campbell et al., 2014). In contrast, some other γ-crystallins have molecular dipoles which do not add in the same way when modelled into the QR interface and which may be oriented towards each other in this configuration which could inhibit even transient monomer- monomer association.

While β-crystallins and chicken γS share characteristics compatible with aligning monomers in the QR configuration, the strength of the interaction depends on other factors: thus, some QR interfaces are clearly non-covalently bonded dimers while others are non-bonded contacts that would be transient in solution. Indeed, AUC confirms that chicken γS shows little evidence for dimer formation in solution.

Thus, it seems that γ-crystallins in general, and γS in particular, have evolved from the β-crystallin template to give monomeric proteins with a molecular surface that confers high solubility without the need for high hydration and allows close molecular contact without multimer formation or aggregation. This suggests a role for γ-crystallins as intermolecular spacers or substitutes for bulk solvent in the crowded lens cytoplasm, helping to maintain both the short-range order necessary for transparency and density of packing necessary for refraction.

Star Methods

Contact for Reagent and Resource Sharing

Further information and requests for reagents should be directed to and will be fulfilled by the Lead Contact, Graeme Wistow (graeme@helix.nih.gov)

EXPERIMENTAL MODEL AND SUBJECT DETAILS

Expression plasmids (pET17b: EMD Millipore, Darmstadt, Germany) in *E. coli* Bl21 Star-DE3 (Thermo Fisher Scientific, Waltham MA) were grown in LB broth (Thermo Fisher Scientific) culture containing 100 μg/ml ampicillin at 37 °C

Methods Details

Protein Expression—Both L16 and Q16 versions of full-length chicken γS crystallin, cloned into the pET17b vector (EMD Millipore, Darmstadt, Germany) (Chen et al., 2016), were expressed in *E. coli* Bl21 Star-DE3 (Thermo Fisher Scientific, Waltham MA). Starter cultures were inoculated into LB broth (Thermo Fisher Scientific) culture containing 100 μg/ml ampicillin at 37 °C, grown to OD_{600} 0.8 and induced with 1 mM IPTG for overnight expression at 20°C. The cells were collected by centrifugation at 5,000 rpm. for 30 min and stored frozen at −80 °C. Frozen pellets were resuspended in buffer A (50 mM imidazole, pH 6.0, 1mM EDTA, 1mM DTT). After resuspension, 0.1 mg of lysozyme/ml was added and incubated at 4 °C for 30 min. The cell suspension was sonicated and the lysate was centrifuged at 16,000 rpm. for 1 h. The supernatant was filtered through a Corning 0.22 μm bottle top filter (Thermo Fisher Scientific), then passed over a 5mL HiTrap SP FFTM (GE Healthcare Life Sciences, Marlborough, MA) pre-equilibrated with Buffer A. Buffer B (50 mM imidazole pH 6.0, 1mM DTT, 1mM EDTA) was used to elute the protein. Protein fractions were pooled and concentrated, then loaded onto a HiLoad 16/60 Superdex 75 pg (GE Healthcare Life Sciences) gel filtration column equilibrated with Buffer C (50mM Tris, pH 7.5, 1mM DTT). Peak fractions were pooled and concentrated for crystallization.

Crystallization—Purified recombinant proteins were crystallized by the sitting-drop vapor-diffusion method. The chicken γS crystallin protein samples were screened for

crystallization conditions using commercially available crystal screens: Index (Hampton Research, Aliso Viejo, CA), PEG/Ion:PEG/Ion 2 (Hampton Research), and Pi-minimal Screen (Jena Bioscience, Ann Arbor MI). A total of 288 conditions were tested in 2μl drops. Screens were incubated at 20°C. The condition producing the largest, most uniform crystal for L16 was selected for optimization. Diffraction quality crystals were obtained initially in 0.2 M Ammonium acetate, pH 7.1, 20% (w/v) PEG 3350. In optimized conditions, (0.2 M Ammonium acetate pH 7.1 and 16% PEG 3350), crystals grew large enough for X-ray diffraction studies after 4–5 days at 20°C.

X-ray analysis—Chicken γS crystals were flash-frozen in mother liquor containing 20% ethylene glycol. Diffraction data were collected at 100K with a rotating copper anode MicroMax 007HF generator equipped with a Saturn A200 CCD detector (Rigaku Americas, The Woodlands, TX) at NIDDK, National Institutes of Health. X-ray data collection and refinement statistics are shown in Table 1. Data were collected out to 2.1 Å, however, because of detector geometry, shells were only complete up to 2.3 Å. Data were collected for 360° with 0.5° oscillation, and gave mosaicity of 0.964. The data were integrated and merged using XDS (Kabsch, 2010). The structure of chicken γS crystallin was solved by molecular replacement using the NMR structure of mouse γS crystallin (PDB ID 1ZWO). The first of the NMR ensemble structures was used, with non-identical residues substituted with glycine. Molecular replacement was performed using the Phaser MR program (McCoy et al., 2007) from the Phenix crystallography software suite 36 (Adams et al., 2010). Rfree was monitored by using 5% of the reflections as a test set. The Z-scores were RFZ=4.7; LLG=94; TFZ=10.1. Structure was refined with TLS with one monomer using Phenix.refine (Adams et al., 2010). The structure is deposited as PDB ID 5VH1.

Informatics—Figures were created using PyMOL (Schrödinger LLC, Cambridge MA). Structure alignments were performed using Align in PyMOL. Surface accessible areas were calculated using NACESS V2.1.1 [http://www.bioinf.manchester.ac.uk/naccess/]. Sequence alignments were performed using Clustal Omega [http://www.ebi.ac.uk/Tools/msa/clustalo/]. Lattice interactions were determined using PISA (Krissinel and Henrick, 2007) and contact residue lists using Contact in CCP4 (Winn et al., 2011). For calculation of molecule dipoles, any missing peptides in β-crystallin structures were model built into x-ray crystal structures using similar regions of other crystallin structures. PDB to PQR in Chimera (Pettersen et al., 2004) was used to generate a PQR file using an Amber force field and a pH of 7.0. The net dipole vector was calculated using Chimera's dipole.py program.

Analytical Ultracentrifugation—Sedimentation velocity (SV) experiments were performed using an Optima XLI/A analytical ultracentrifugation (Beckman Coulter, Indianapolis, IN), following previously described standard protocols (Schuck, 2016; Schuck et al., 2015). Briefly, 100 μL of chromatographically purified protein samples in 50 mM Tris-HCl and 1 mM DTT, pH 8.5, at concentrations between 2.9 and 24 mg/ml were inserted in cell assemblies with 3 mm Epon double-sector centerpieces and sapphire windows, and sedimented at 50,000 rpm in an An50 Ti rotor at 20.3 °C. Interference data were fitted using the c(s) continuous sedimentation coefficient distribution with the software SEDFIT (Schuck, 2000, 2016). The distributions were integrated to determine weight-average

sedimentation coefficients sw, and the isotherm sw as a function of protein concentration was modeled in SEDPHAT with monomer-dimer models including hydrodynamic non-ideality (Patel et al., 2007; Schuck, 2003). In this model, the sedimentation coefficient of the dimer was constrained to between 1.4 – 1.6fold that of the monomer, and the hydrodynamic non-ideality coefficient ks was fixed to the 0.0083 ml/mg on the basis of the hydrodynamic theory for the hydrodynamically equivalent sphere (Batchelor, 1972).

Sedimentation equilibrium (SE) experiments were carried out at rotor speeds of 12,000, 16,000, and 25,000 rpm at a temperature of 4 °C using a time-optimized over speeding protocol (Ma et al., 2015). Absorbance data at 278 nm were acquired for 3 samples at loading concentrations between 2.3 – 17 μM. Solution density was calculated using SEDNTERP (Laue et al., 1992), and the partial-specific volume was based on amino acid composition in SEDFIT using the Cohn-Edsall tables (Cohn and Edsall, 1943). SE profiles were globally fit in SEDPHAT to a single-species model with implicit mass conservation (Vistica et al., 2004).

Data and Software Availability

Atomic coordinates and structure factors for chicken γS-crystallin are deposited in the Protein Data Bank under the accession code 5VH1.

Supplementary Material

Refer to Web version on PubMed Central for supplementary material.

Acknowledgments

This work was supported by the Intramural Program of the National Eye Institute and the National Institute of Biomedical Imaging and Bioengineering. We thank Dr. Fred Dyda for facilitating use of the diffraction equipment in the Molecular Structure Section at the NIDDK, National Institutes of Health and for help in data collection.

References

Adams PD, Afonine PV, Bunkoczi G, Chen VB, Davis IW, Echols N, Headd JJ, Hung LW, Kapral GJ, Grosse-Kunstleve RW, et al. PHENIX: a comprehensive Python-based system for macromolecular structure solution. Acta Crystallogr D Biol Crystallogr. 2010; 66:213–221. [PubMed: 20124702]

Basak AK, Kroone RC, Lubsen NH, Naylor CE, Jaenicke R, Slingsby C. The C-terminal domains of gammaS-crystallin pair about a distorted twofold axis. Protein Eng. 1998; 11:337–344. [PubMed: 9681865]

Batchelor GK. Sedimentation in a dilute dispersion of spheres. J Fluid Mech. 1972; 52:245–268.

Bateman OA, Lubsen NH, Slingsby C. Association behaviour of human betaB1-crystallin and its truncated forms. Experimental Eye Research. 2001; 73:321–331. [PubMed: 11520107]

Bax B, Lapatto R, Nalini V, Driessen H, Lindley PF, Mahadevan D, Blundell TL, Slingsby C. X-ray analysis of betaB2-crystallin and evolution of oligomeric lens proteins. Nature. 1990; 347:776–780. [PubMed: 2234050]

Blundell T, Lindley P, Miller L, Moss D, Slingsby C, Tickle I, Turnell B, Wistow G. The molecular structure and stability of the eye lens: x-ray analysis of gamma-crystallin II. Nature. 1981; 289:771–777. [PubMed: 7464942]

Campbell B, Petukh M, Alexov E, Li C. On the electrostatic properties of homodimeric proteins. Journal of theoretical & computational chemistry. 2014:13.

Chen Y, Sagar V, Len HS, Peterson K, Fan J, Mishra S, McMurtry J, Wilmarth PA, David LL, Wistow G. gamma-Crystallins of the chicken lens: remnants of an ancient vertebrate gene family in birds. FEBS J. 2016; 283:1516–1530. [PubMed: 26913478]

Chen Y, Zhao H, Schuck P, Wistow G. Solution properties of gamma-crystallins: compact structure and low frictional ratio are conserved properties of diverse gamma-crystallins. Protein Sci. 2014; 23:76–87. [PubMed: 24214907]

Cohn, EJ., Edsall, JT. Proteins, amino acids and peptides as ions and dipolar ions. New York: Reinhold Publishing Corporation; 1943.

Delaye M, Tardieu A. Short-range order of crystallin proteins accounts for eye lens transparency. Nature. 1983; 302:415–417. [PubMed: 6835373]

Evans P, Wyatt K, Wistow GJ, Bateman OA, Wallace BA, Slingsby C. The P23T Cataract Mutation Causes Loss of Solubility of Folded gammaD-Crystallin. J Mol Biol. 2004; 343:435–444. [PubMed: 15451671]

Fan J, Dong L, Mishra S, Chen Y, Fitzgerald P, Wistow G. A role for gammaS-crystallin in the organization of actin and fiber cell maturation in the mouse lens. FEBS J. 2012; 279:2892–2904. [PubMed: 22715935]

Kabsch W. XDS. Acta Crystallogr D Biol Crystallogr. 2010; 66:125–132. [PubMed: 20124692]

Kappe G, Purkiss AG, van Genesen ST, Slingsby C, Lubsen NH. Explosive expansion of betagamma-crystallin genes in the ancestral vertebrate. J Mol Evol. 2010; 71:219–230. [PubMed: 20725717]

Krissinel E, Henrick K. Inference of macromolecular assemblies from crystalline state. J Mol Biol. 2007; 372:774–797. [PubMed: 17681537]

Lapatto R, Nalini V, Bax B, Driessen H, Lindley PF, Blundell TL, Slingsby C. High resolution structure of an oligomeric eye lens beta-crystallin. Loops, arches, linkers and interfaces in betaB2 dimer compared to a monomeric gamma-crystallin. Journal of Molecular Biology. 1991; 222:1067–1083. [PubMed: 1762146]

Laue, TM., Shah, BD., Ridgeway, TM., Pelletier, SL. Computer-aided interpretation of analytical sedimentation data for proteins. In: Harding, SE.Rowe, AJ., Horton, JC., editors. Anal Ultracentrifugation Biochem Polym Sci. Cambridge: The Royal Society of Chemistry; 1992. p. 90-125.

Ma J, Metrick M, Ghirlando R, Zhao H, Schuck P. Variable-Field Analytical Ultracentrifugation: I. Time-Optimized Sedimentation Equilibrium. Biophys J. 2015; 109:827–837. [PubMed: 26287634]

Mahendiran K, Elie C, Nebel JC, Ryan A, Pierscionek BK. Primary sequence contribution to the optical function of the eye lens. Sci Rep. 2014; 4:5195. [PubMed: 24903231]

McCoy AJ, Grosse-Kunstleve RW, Adams PD, Winn MD, Storoni LC, Read RJ. Phaser crystallographic software. J Appl Crystallogr. 2007; 40:658–674. [PubMed: 19461840]

Mohr BG, Dobson CM, Garman SC, Muthukumar M. Electrostatic origin of in vitro aggregation of human γ-crystallin. The Journal of Chemical Physics. 2013; 139:121914. [PubMed: 24089726]

Norledge BV, Hay RE, Bateman OA, Slingsby C, Driessen HP. Towards a molecular understanding of phase separation in the lens: a comparison of the X-ray structures of two high Tc gamma-crystallins, gammaE and gammaF, with two low Tc gamma-crystallins, gammaB and gammaD. Exp Eye Res. 1997; 65:609–630. [PubMed: 9367641]

Pande A, Mokhor N, Pande J. Deamidation of Human gammaS-Crystallin Increases Attractive Protein Interactions: Implications for Cataract. Biochemistry. 2015; 54:4890–4899. [PubMed: 26158710]

Patel TR, Harding SE, Ebringerova A, Deszczynski M, Hromadkova Z, Togola A, Paulsen BS, Morris GA, Rowe AJ. Weak self-association in a carbohydrate system. Biophys J. 2007; 93:741–749. [PubMed: 17483161]

Pettersen EF, Goddard TD, Huang CC, Couch GS, Greenblatt DM, Meng EC, Ferrin TE. UCSF Chimera--a visualization system for exploratory research and analysis. J Comput Chem. 2004; 25:1605–1612. [PubMed: 15264254]

Purkiss AG, Bateman OA, Goodfellow JM, Lubsen NH, Slingsby C. The X-ray crystal structure of human gamma S-crystallin C-terminal domain. Journal of Biological Chemistry. 2002; 277:4199–4205. [PubMed: 11706012]

Purkiss AG, Bateman OA, Wyatt K, Wilmarth PA, David LL, Wistow GJ, Slingsby C. Biophysical properties of gammaC-crystallin in human and mouse eye lens: the role of molecular dipoles. J Mol Biol. 2007; 372:205–222. [PubMed: 17659303]

Quax-Jeuken Y, Driessen H, Leunissen J, Quax W, de Jong W, Bloemendal H. beta s-Crystallin: structure and evolution of a distinct member of the beta gamma-superfamily. EMBO J. 1985; 4:2597–2602. [PubMed: 4054100]

Ray ME, Wistow G, Su YA, Meltzer PS, Trent JM. AIM1, a novel non-lens member of the betagamma-crystallin superfamily, is associated with the control of tumorigenicity in human malignant melanoma. Proc Natl Acad Sci U S A. 1997; 94:3229–3234. [PubMed: 9096375]

Ray NJ, Hall D, Carver JA. Deamidation of N76 in human gammaS-crystallin promotes dimer formation. Biochim Biophys Acta. 2016; 1860:315–324. [PubMed: 26318015]

Schuck P. Size-distribution analysis of macromolecules by sedimentation velocity ultracentrifugation and lamm equation modeling. Biophys J. 2000; 78:1606–1619. [PubMed: 10692345]

Schuck P. On the analysis of protein self-association by sedimentation velocity analytical ultracentrifugation. Anal Biochem. 2003; 320:104–124. [PubMed: 12895474]

Schuck, P. Sedimentation Velocity Analytical Ultracentrifugation: Discrete Species and Size-Distributions of Macromolecules and Particles. Boca Raton: CRC Press; 2016.

Schuck, P., Zhao, H., Brautigam, CA., Ghirlando, R. Principles of Analytical Ultracentrifugation. Boca Raton, FL: CRC Press; 2015.

Slingsby C, Wistow GJ. Functions of crystallins in and out of lens: Roles in elongated and post-mitotic cells. Prog Biophys Mol Biol. 2014; 115:52–67. [PubMed: 24582830]

Slingsby C, Wistow GJ, Clark AR. Evolution of crystallins for a role in the vertebrate eye lens. Protein Sci. 2013; 22:367–380. [PubMed: 23389822]

Smith MA, Bateman OA, Jaenicke R, Slingsby C. Mutation of interfaces in domain-swapped human betaB2-crystallin. Protein Sci. 2007; 16:615–625. [PubMed: 17327390]

Tardieu A, Veretout F, Krop B, Slingsby C. Protein interactions in the calf eye lens: interactions between beta-crystallins are repulsive whereas in gamma-crystallins they are attractive. European biophysics journal: EBJ. 1992; 21:1–12. [PubMed: 1516556]

Teichmann U, Ray ME, Ellison J, Graham C, Wistow G, Meltzer PS, Trent JM, Pavan WJ. Cloning and tissue expression of the mouse ortholog of AIM1, a betagamma-crystallin superfamily member. Mamm Genome. 1998; 9:715–720. [PubMed: 9716656]

Van Montfort RL, Bateman OA, Lubsen NH, Slingsby C. Crystal structure of truncated human betaB1-crystallin. Protein Sci. 2003; 12:2606–2612. [PubMed: 14573871]

Vistica J, Dam J, Balbo A, Yikilmaz E, Mariuzza RA, Rouault TA, Schuck P. Sedimentation equilibrium analysis of protein interactions with global implicit mass conservation constraints and systematic noise decomposition. Anal Biochem. 2004; 326:234–256. [PubMed: 15003564]

Winn MD, Ballard CC, Cowtan KD, Dodson EJ, Emsley P, Evans PR, Keegan RM, Krissinel EB, Leslie AG, McCoy A, et al. Overview of the CCP4 suite and current developments. Acta Crystallogr D Biol Crystallogr. 2011; 67:235–242. [PubMed: 21460441]

Wistow G. The human crystallin gene families. Hum Genomics. 2012; 6:26. [PubMed: 23199295]

Wistow G, Turnell B, Summers L, Slingsby C, Moss D, Miller L, Lindley P, Blundell T. X-ray analysis of the eye lens protein gamma-II crystallin at 1.9 A resolution. J Mol Biol. 1983; 170:175–202. [PubMed: 6631960]

Wistow G, Wyatt K, David L, Gao C, Bateman O, Bernstein S, Tomarev S, Segovia L, Slingsby C, Vihtelic T. gammaN-crystallin and the evolution of the betagamma-crystallin superfamily in vertebrates. FEBS J. 2005; 272:2276–2291. [PubMed: 15853812]

Wu Z, Delaglio F, Wyatt K, Wistow G, Bax A. Solution structure of (gamma)S-crystallin by molecular fragment replacement NMR. Protein Sci. 2005; 14:3101–3114. [PubMed: 16260758]

Xi Z, Whitley MJ, Gronenborn AM. Human betaB2-Crystallin Forms a Face-en-Face Dimer in Solution: An Integrated NMR and SAXS Study. Structure. 2017

Zhao H, Brown PH, Magone MT, Schuck P. The molecular refractive function of lens gamma-Crystallins. J Mol Biol. 2011a; 411:680–699. [PubMed: 21684289]

Zhao H, Chen Y, Rezabkova L, Wu Z, Wistow G, Schuck P. Solution properties of gamma-crystallins: hydration of fish and mammal gamma-crystallins. Protein Sci. 2014; 23:88–99. [PubMed: 24282025]

Zhao H, Magone MT, Schuck P. The role of macromolecular crowding in the evolution of lens crystallins with high molecular refractive index. Phys Biol. 2011b; 8:046004. [PubMed: 21566271]

Highlights

- Crystal structure of γS-crystallin sheds light on contacts in the crowded eye lens
- Monomeric γS forms a non-bonding lattice contact like dimeric β-crystallins
- Common interface conserves orientation but only one conserved side-chain contact
- Common interface is associated with similar patterns of molecular dipoles

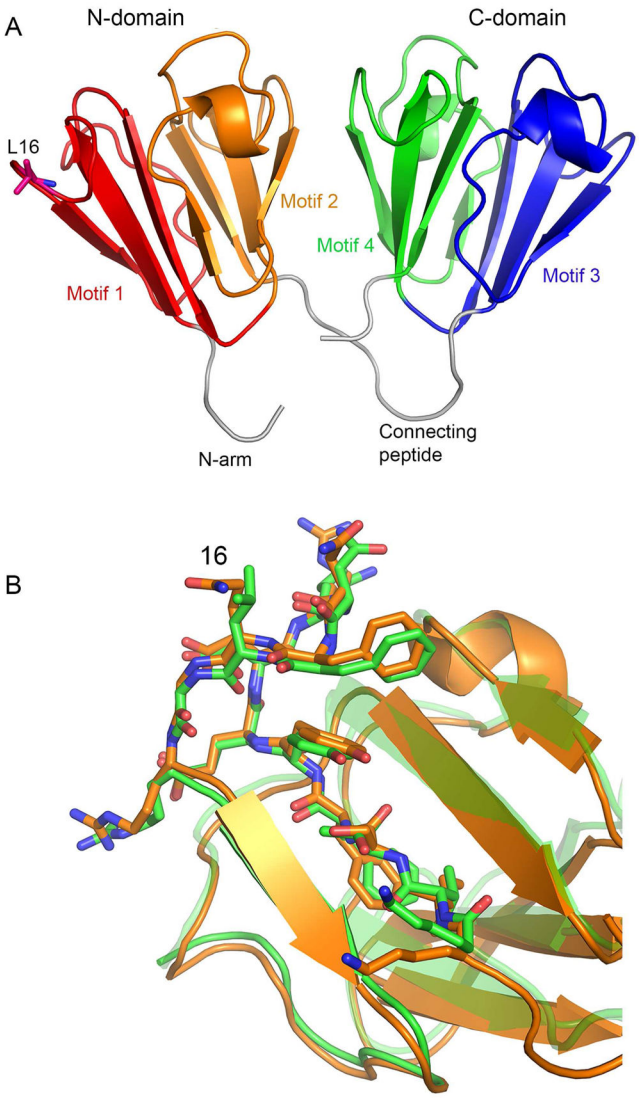

Figure 1. Structure of Chicken γS-crystallin

A: Main chain trace and secondary structure elements. Repeated motif and domain structures are labelled.

B: Alignment of residues around position 16 in the chicken crystal structure and the mouse NMR structure for γS. The Q>L substitution has little effect on local structure.

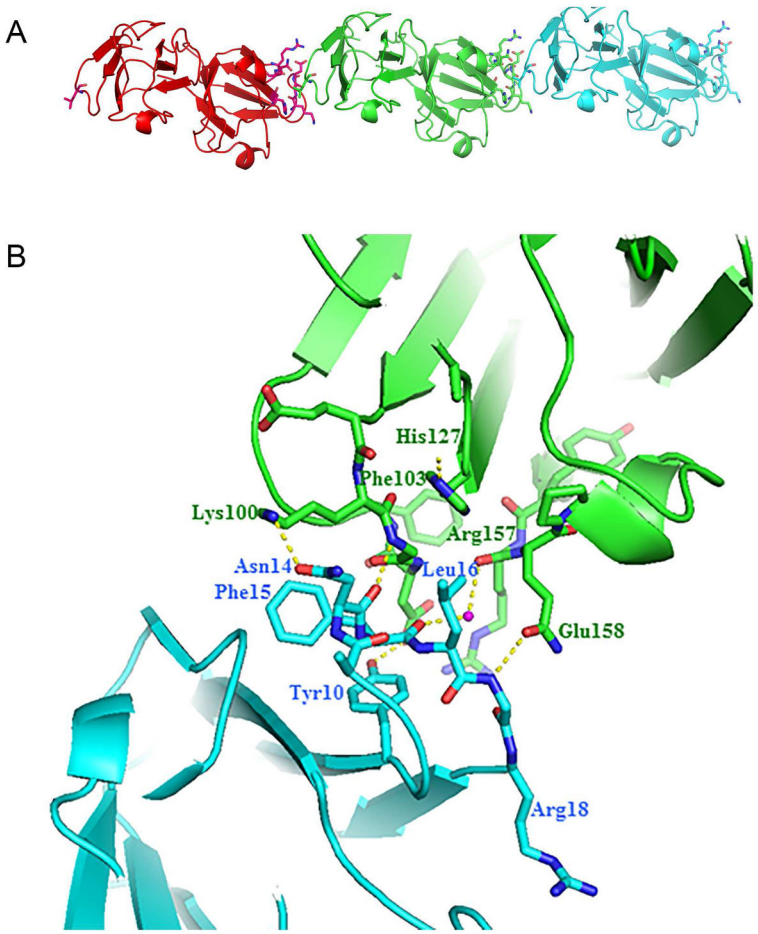

Figure 2. Lattice contact involving L16

A: Overview of monomer to monomer contact in the crystal lattice centered on L16.

B: Detailed view of contact. L16 makes no direct hydrophobic contact but is substantially shielded from water by the neighboring monomer. Several intermolecular hydrogen bonds are shown between monomers in blue and green.

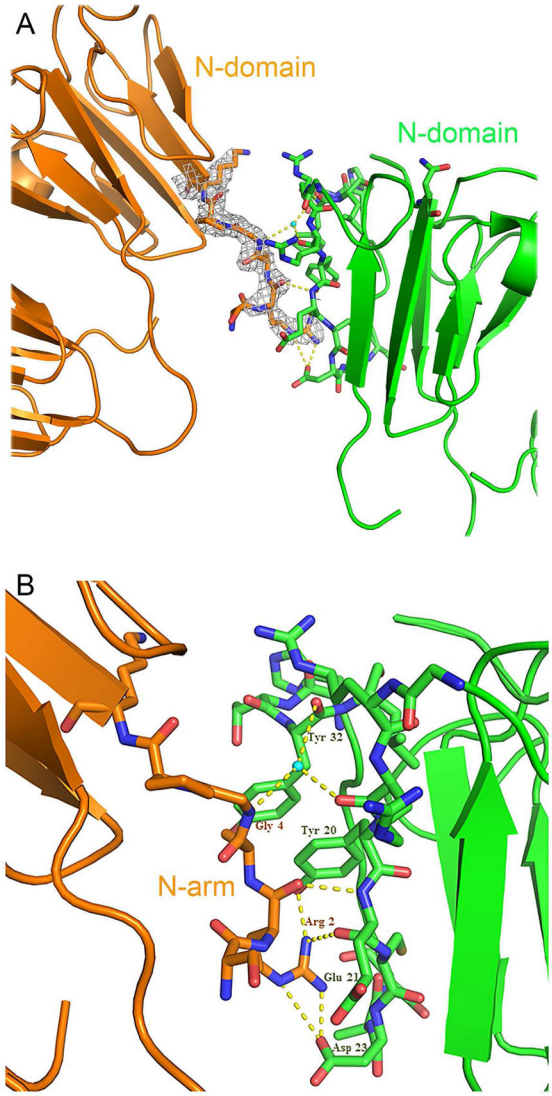

Figure 3. Lattice contact involving the N-arm

A: The N-arm aligns with the edge of a β-sheet of the N-domain of another monomer. The well-defined electron density for the N-arm is shown.

B: A closer view of the lattice contact shows hydrogen bonding between monomers. There is one main chain backbone hydrogen bond interaction, between the peptide carbonyl of R2 and the peptide nitrogen of the adjacent Q21′ while a second interaction between G4 and R19′ is bridged by water. The side chain of R2 forms an ion-pair with D23′of the other monomer and is within hydrogen bonding distance of Y20′.

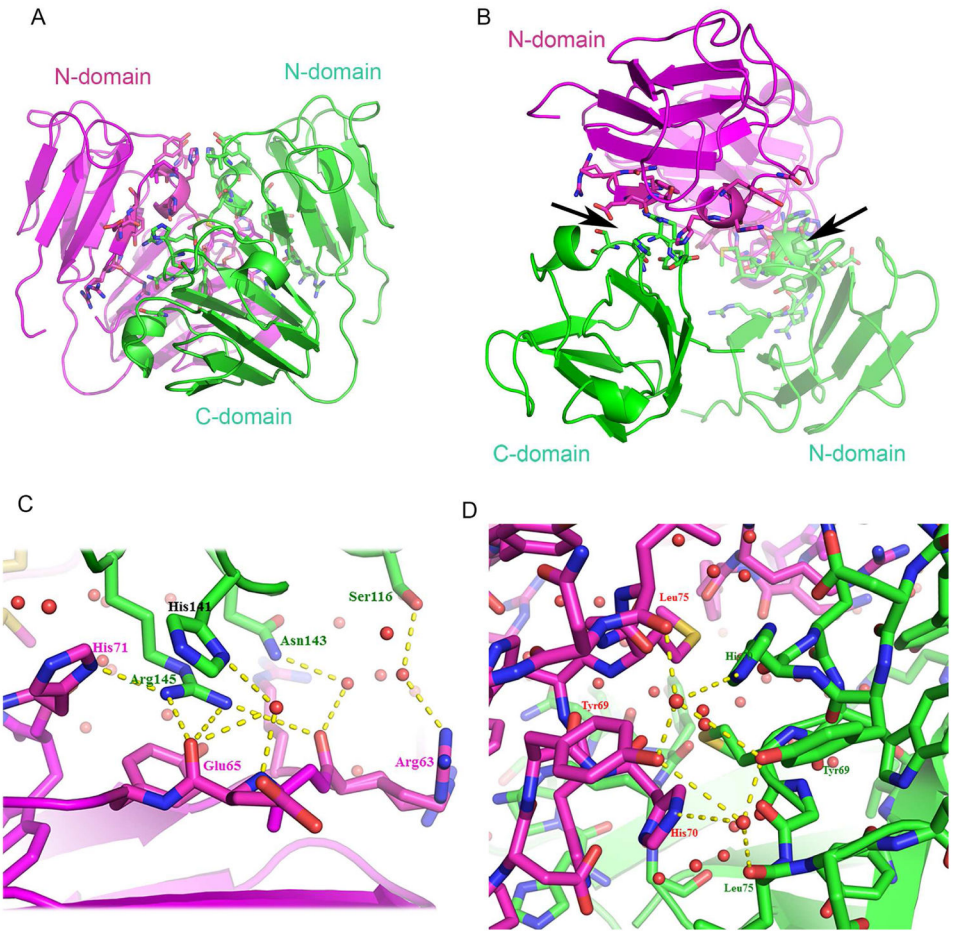

Figure 4. A large lattice contact between γS monomers contains tightly coordinated water

A, B: Two views of the monomer- monomer (red and green) contact are shown in secondary structure trace, with residues in the contact region shown as stick models. The contact involves two groups of residues from interdomain motifs 2 and 4 of the symmetry related neighbors. Contact residues are indicated with arrows in view B. C: Surface polar side chains in the lattice contact form networks including a thin layer of tightly bound water (red spheres). There are direct side chain interactions, such as His71-Arg145 and water bridges such as Arg63-Ser116. D: Another region showing tightly bound waters and water bridges. Hydrogen bonds are shown as dotted lines.

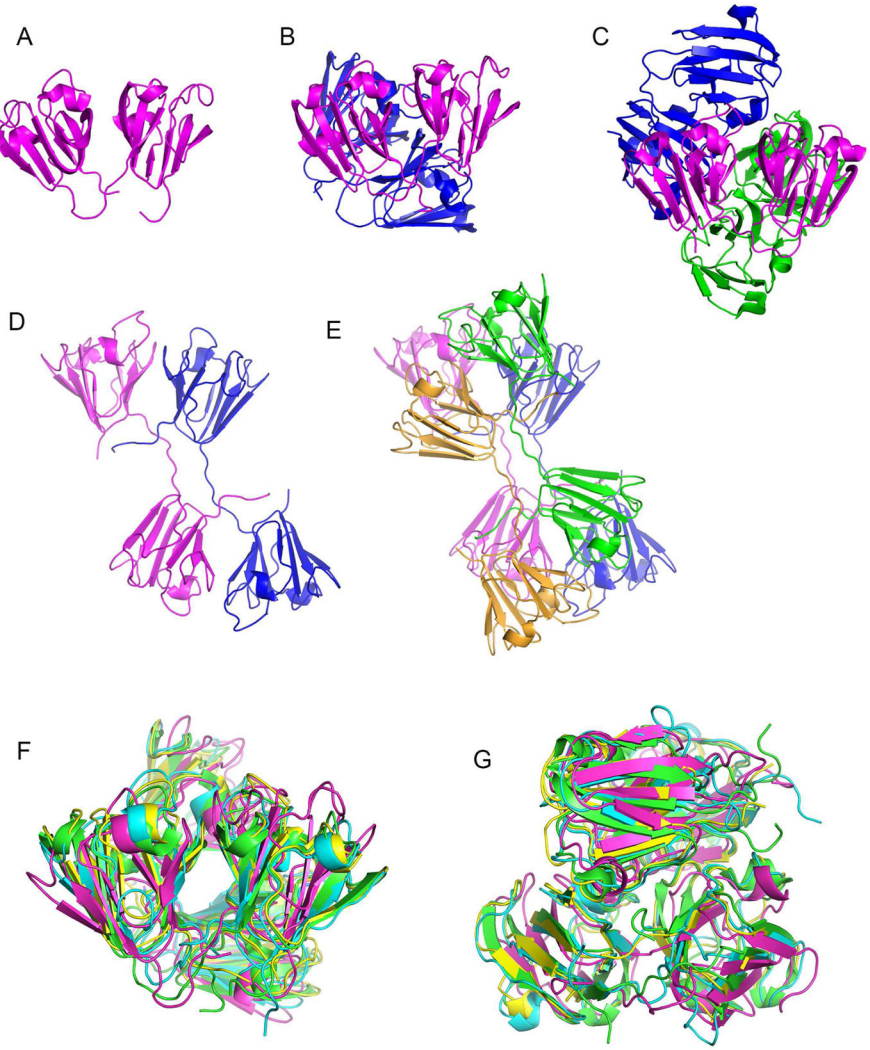

Figure 5. Conserved dimer-like interaction among β-crystallins and γS-crystallin

A–E show ribbon traces to illustrate different arrangements of monomeric γ-crystallins and multimeric β-crystallins in crystal structures. A: chicken γS monomer. B: human βB1 dimer with QR interface. C: human βB3 trimer. D: human βB2 domain-swapped dimer. E: The non-bonded crystal lattice tetramer of human βB2. F and G: Two views of a structural alignment of crystal dimeric or monomer-monomer interactions about the QR interface for γS (red), βB1 (green), βB2 (yellow) and βA4 (blue).

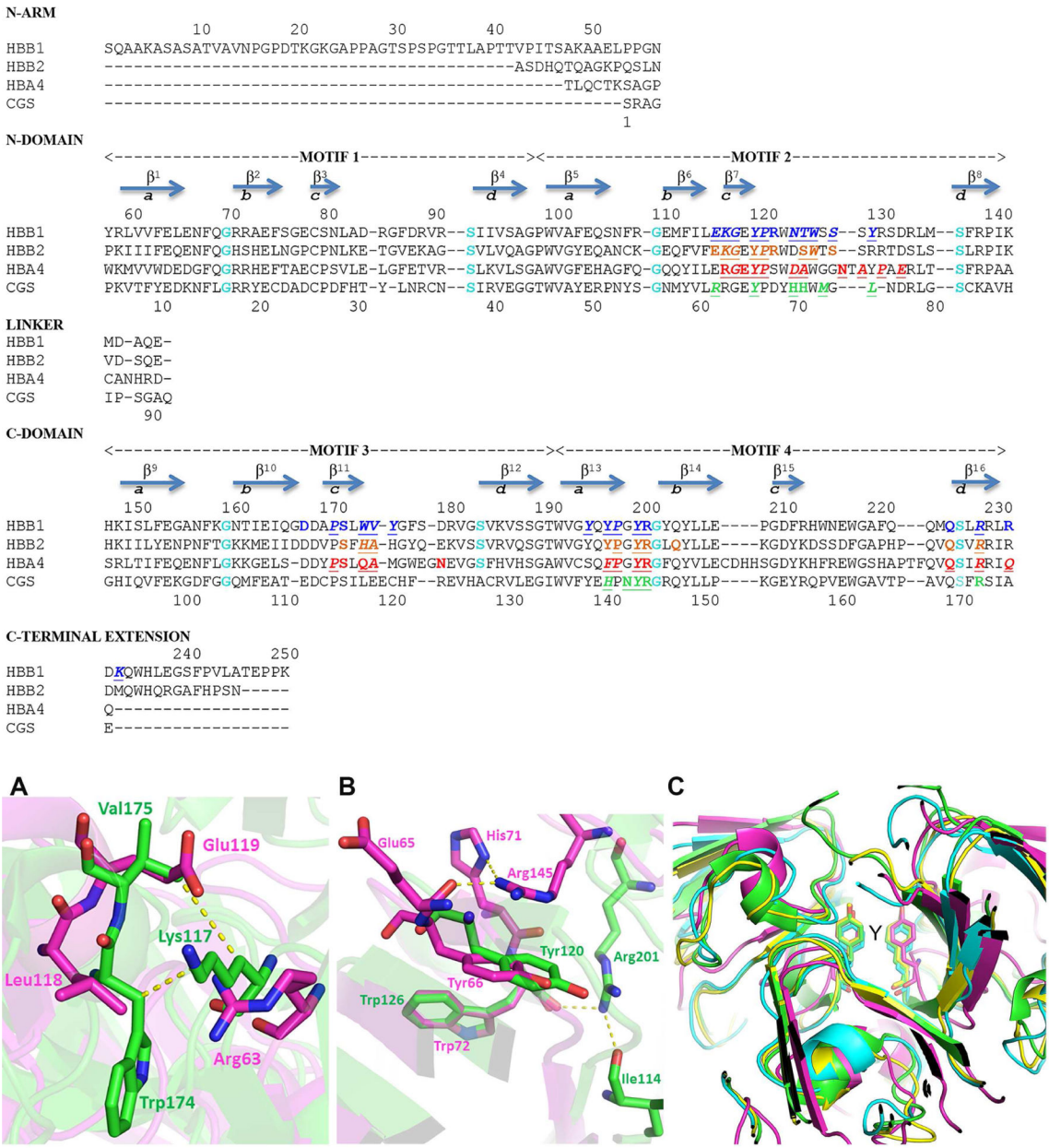

Figure 6. Residues of the QR interface

Top: Sequence alignment of β- and γ-crystallins exhibiting the QR interface. Human βB1 (GenBank: AAC50383.1); Human βB2 (GenBank: AB25691.1); Human βA4 (GenBank: AAC50970.1) Chicken γS (GenBank: ACX94083.1). Initiator methionines are not included in alignment or numbering. Protein sequences are aligned to emphasize the common four motif structure with the important G and S residues in blue. General positions of β-strands are indicated with *a, b, c, d* indicating the four strands of each motif. Residues involved in the QR interface, as defined by Contact are shown colored. Sequence positions are given for βB1 (above) and γS (below). Details of contacts are listed in Table S2. Below: Only one residue is completely conserved in the different QR interfaces. A: An example of a non-polar contact in the βB1 dimer (green) that is not present in the chicken γS QR interface

(red). B: Arg145 of γS (red) and Arg201 of βB1 (green) are conserved, but adopt different conformations in the two proteins. C: Tyr144 (of γS) is completely conserved in all QR interfaces. A multiple alignment of γS and β-crystallin structures with the QR interface shows the close superposition of the conserved tyrosine equivalent to Y144 in γS (Y). Colors are as in fig 5.

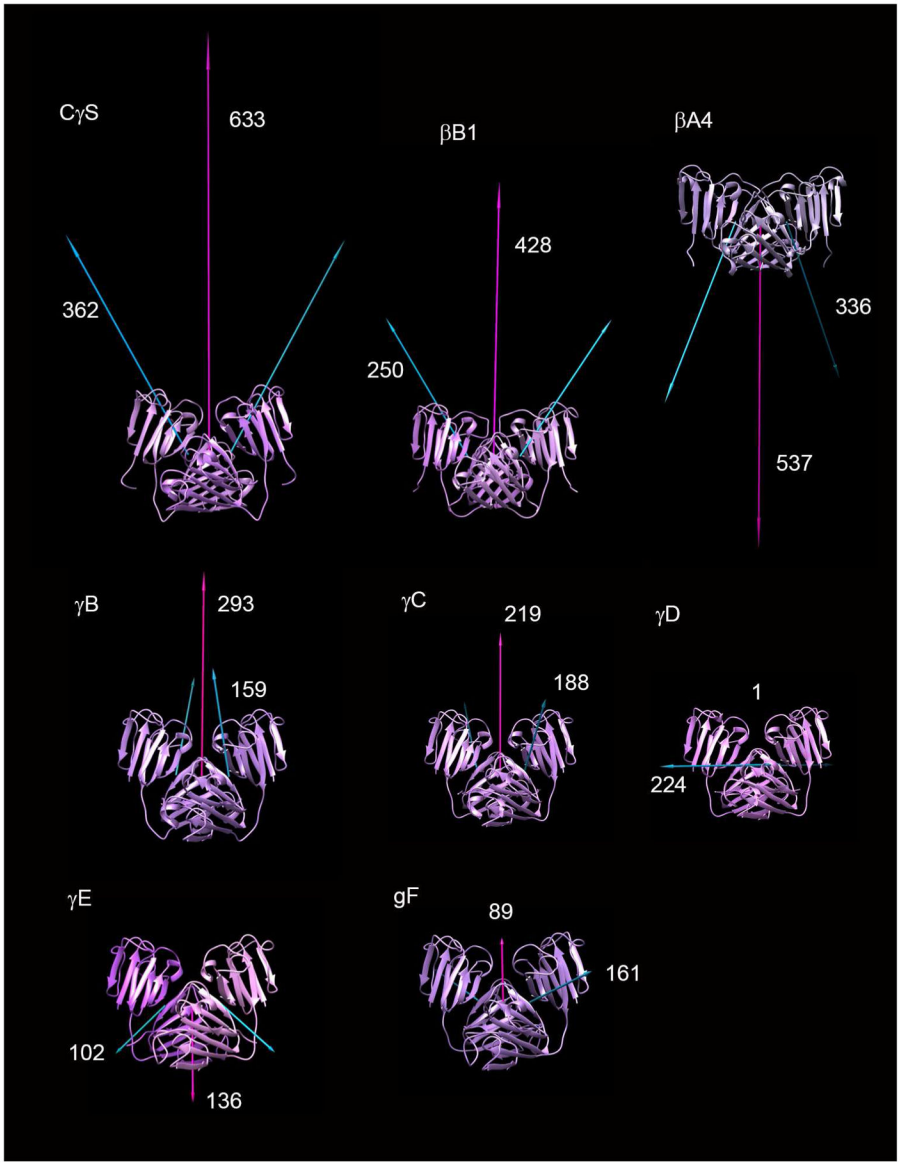

Figure 7. Proteins which adopt QR have similar aligned and additive molecular dipoles

QR interactions for crystal and modelled structures for β- and γ-crystallins are shown in the same orientation. Calculated molecular dipole moments for monomers are shown as white vectors; dipoles for the dimer are shown in red. Magnitudes (in Debye units) are indicated by length and by the associated values.

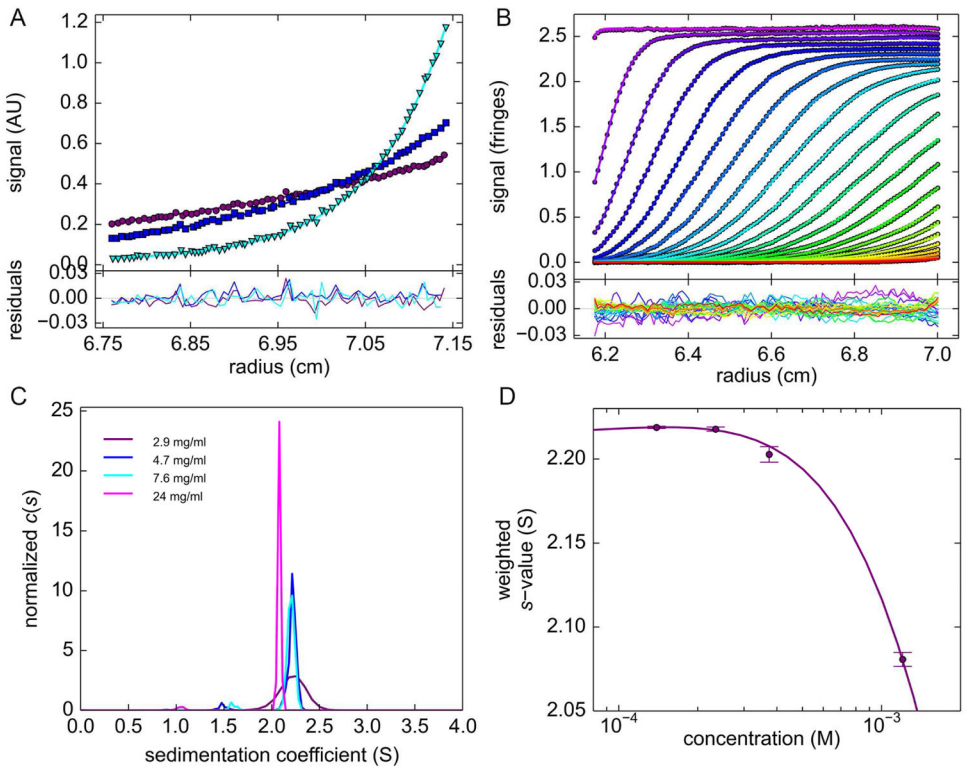

Figure 8. AUC measurements show no evidence for multimer formation by chicken γS

A: Representative sedimentation equilibrium distributions of 7 μM γS at 12,000 (purple), 16,000 (blue) and 25,000 rpm (green). For clarity, only every third data point is shown (symbols). The solid lines are the global fit (including data at other concentrations, not shown) with a single-species model with best-fit molar mass of 20.2 kDa.

B: Sedimentation velocity profiles of 2.9 mg/ml chicken γS at 50,000 rpm (symbols; for clarity, only every 10th data point is shown, and later scans are indicated by higher color temperature), fitted with a c(s) distribution (solid lines). Residuals are shown in the lower panel.

C: Best-fit c(s) distributions obtained from the analysis of sedimentation velocity profiles of chicken γS at different concentrations.

D: Isotherm of experimental weighted-average s-values as a function of concentration (symbols), fitted by using monomer dimer self-association model (solid line) including repulsive hydrodynamic non-ideality, leading to a best-fit KD value of 4.2 mM.

Table 1

Crystallographic Data.

Data collection	
Space group	C2
Cell dimensions	
a, b, c (Å)	86.91, 41.01, 49.46
α, β, γ (°)	90.00, 113.204, 90.00[a]
Resolution (Å)	45.5–2.31 (2.35–2.31)[b]
Rsym	0.053(0.088)[b]
I/σI	27 (4.8)[b]
Completeness (%)	98.5 (86.9)[b]
Redundancy	3.4 (2.1)
Refinement	
Resolution (Å)	34.5–2.30 (2.63–2.30)
No. reflections	19,451 (1,942)
Rwork/Rfree	13.2/20.2 (16.0/27.3)[b]
No. atoms	1,679
Protein	1,472
Ligand/ion	0
Water	154
B factors (average; Å2)	25.9
Protein	25.3
Water	31.6
R.m.s. deviations	
Bond lengths (Å)	0.007
Bond angles (°)	0.94

[a] One crystal was used for each data set.

[b] Values in parentheses are for highest-resolution shell.

Table 2

Lattice contacts from PISA

Data for the six lattice contacts for chicken γS determined by PISA. Mon1/2# Atoms -Number of interfacing atoms for monomer 1/2. Mon1/2# Residues -Number of interfacing residues for monomer ½. N_{HB}: Number of hydrogen bonds. $N_{sb:}$ Number of salt bridges. $N_{DB:}$ Number of disulfide bonds. G: calculated free energy for interaction.

	Mon1# Atoms	Mon1# Residues	Symmetry Operation	Mon2# Atoms	Mon2# Residues	Area, A^2	G kcal/mol	N_{HB}	N_{SB}	N_{DS}	Comment
1	95	26	-x, **y**,-z+1	95	26	851.7	4.7	9	2	0	QR Dimer
2	39	11	x-1/2, y+1/2, z	42	11	389.8	2.4	7	1	0	L16
3	24	7	-x-1/2, y-**1**/2,-z	35	10	247.1	1.5	4	2	0	N-arm
4	25	6	x, y-1, z	22	8	211.4	1.2	3	0	0	
5	26	10	-**x**, y,-z	26	10	208.7	−2.7	2	2	0	
6	8	4	-x+1/2, y-1/**2**, -z+1	7	6	64.4	0.1	0	0	0	